A Model Reduction Method for a Class of 2-D Systems

Mahmood R. Azimi-Sadjadi, *Senior Member, IEEE,* and Khashayar Khorasani, *Member, IEEE*

Abstract—A decomposition-aggregation scheme for reduction of dimensionality for a class of 2-D systems is introduced. This method, which is based upon the extension of the singular perturbation method in two dimensions, is used to decompose the original 2-D system into two reduced-order 2-D subsystems. These reduced order subsystems are shown to effectively capture the dynamical behavior of the original full-order system. Two numerical examples are provided that indicate the effectiveness of this method when used in image modeling applications.

I. INTRODUCTION

PARAMETRIC representation of images involves fitting an appropriate autoregressive (AR) or autoregressive moving average (ARMA) model to the image that would realize the given covariance function or equivalently the spectral density function of the relevant image. The mismatch between the covariances generated by the model and those of the original image field can be reduced by increasing the order of the model. On the other hand, the principle of parsimony precludes the use of a model having a large number of parameters. It is, therefore, desirable to develop a model reduction scheme that can be applied to the original full-order model to obtain the relevant reduced-order models that preserve the stability and correlation properties of the original system. These reduced-order subsystems can then be used in place of the full-order system for synthesis and analysis problems.

Model reduction for 2-D systems described by state-space formulations has been considered in a number of recent papers [1]–[6]. Jury and Premaratne [1] extended the 1-D model reduction technique of Badreddin and Mansour [2] to the 2-D case. However, unfortunately, in contrast to the 1-D case, in the 2-D extension the stability of the reduced-order system is not generally guaranteed even for a stable full-order system. Lu, Lee, and Zhang [3] developed a model reduction method using a generalized balanced realization that exploits the properties of the reachability and observability Grammians. For a balanced realization these Grammians provide

measure of couplings of input-to-state and state-to-output. The effects of weakly coupled states are ignored in this method. In the method proposed by Zilouchian and Carroll [4], structure transformations are applied to the full-order system to reduce the number of vertical and horizontal states separately. The transformation matrices are determined such that the error between the outputs of the full-order and reduced-order systems is minimized. Balanced realization is suggested to provide a good minimization procedure. More recently, Premaratne *et al.* [5] have extended their method to the 2-D multi-input multi-output case. In [6], they have obtained new results on the stability, minimality, and Grammian computation for separable 2-D systems.

In our earlier work [7], [8], the singular perturbation method was used for order reduction of 1-D and 2-D dynamic models of images. In [7], this method is employed to derive a reduced-order strip Kalman filter for image restoration applications. The idea of applying singular perturbation for 2-D model reduction was first reported in [8] and then later extended in [9] and [10].

The methodology for model reduction is greatly dependent on the particular choice of model description. In this paper, a new approach for model reduction is presented for a class of 2-D systems described by finite-order 2-D causal difference equations with strong–weak coupling effects within their region of support (ROS). This approach, which is based upon the extension of the singular perturbation methodology, exploits the strong–weak coupling effects between a group of pixels within the ROS to obtain a 2-D image model in singularly perturbed form. This model is arranged into a 2-D state-space realization with "two-time-scale" property (to be specified later; see also [1] and [2]). This property is then used to capture the aggregated effects of the weakly correlated states (pixels) on those strongly correlated ones and hence obtain 2-D reduced-order models, which perform very closely to the original 2-D full-order system. This is accomplished by using the decomposition-aggregation capabilities of the singular perturbation method. This model reduction scheme is used to decompose 2-D systems into slow and fast 2-D subsystems associated, respectively, with the strongly and weakly coupled state variables. The 2-D reduced-order models preserve the dynamic properties of the original 2-D full-order system. Two numerical examples are given, which demonstrate the usefulness and utilities of this method for image modeling applications. The results are compared with those obtained using a conventional image data compression scheme, namely, the Karhunen–Loeve (KL) transform.

II. A 2-D Singularly Perturbed Image Model

Consider a causal linear space-invariant 2-D image model described by the following $M \times M$th-order difference equation with quarter plane ROS,

$$y(m, n) = \sum_{p, q \in W} \alpha_{p,q} y(m - p, n - q) + u(m, n) \quad (1)$$

where $W = \{p, q: 0 \le p \le M, 0 \le q \le M, (p, q) \ne (0, 0)\}$ and $\{u(m, n)\}$ and $\{y(m, n)\}$ represent the input and the output arrays, respectively. Since any general linear space-invariant 2-D recursive system can be viewed as a cascade of a 2-D all-zero system and a 2-D all-pole system, and since the model reduction scheme proposed in this paper does not affect the all-zero part, thus without any loss of generality, we have throughout this work considered only the all-pole systems. (See Section 6.2 for an ARMA modeling example).

Now, let us assume that the ROS, W, of this model is partitioned into two subregions, W_1 and W_2, such that $W_1 \cap W_2 = \emptyset$ and $W_1 \cup W_2 = W$ where the pixels in W_1 are strongly correlated with the present pixel $y(m, n)$, and those in W_2 are weakly correlated with $y(m, n)$. These strong–weak coupling effects between the pixels in the ROS exist due to the local spatial activities within an image. The partitioned ROS is shown in Fig. 1. The coefficients $\alpha_{p,q}$'s of the difference equation (1) in the subregions are assumed to be given by

$$\alpha_{p,q} = a_{p,q}, \quad \text{for} \quad p + q \in [1, N] \quad (2a)$$

$$\alpha_{p,q} = \epsilon^{p+q-N} a_{p,q}, \quad \text{for} \quad p + q \in [N + 1, 2M] \quad (2b)$$

where ϵ is a positive real number greater than zero and normally very much less than one. The choice of the perturbation parameter, ϵ, is discussed in Section III. The above definitions confirm the fact that the pixels in region W_1 are highly correlated to $y(m, n)$ as their corresponding coefficients are of order 1, whereas the pixels in region W_2 are weakly correlated to $y(m, n)$ and their coefficients are of order $\epsilon, \epsilon^2, \cdots, \epsilon^{2M-N}$ when their spatial diagonal distances from $y(m, n)$ are respectively $N + 1, N + 2, \cdots, 2M$ (see Fig. 1). The system described by (1) is now in a 2-D singularly perturbed form in the sense that by formally setting $\epsilon = 0$, the order of the system is reduced from $M \times M$ to $N \times N$. Note that this is different from a regular perturbation problem in the sense that in a regularly perturbed system the order of the system is unchanged when the perturbation parameter is neglected. This is not the case for system (1). By neglecting the perturbation parameter in (1) the reduced-order (truncated) 2-D system becomes

$$y(m, n) = \sum_{p, q \in W_1} a_{p,q} y(m - p, n - q) + u(m, n). \quad (3)$$

Although the reduced-order system (3) provides computational simplicity, it will not generally be able to give a complete representation of the system characteristics. This is
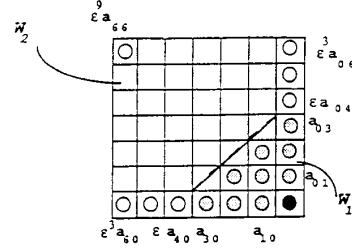

Fig. 1. Region of support of the 2-D AR model and strong and weak coupling regions.

due to the fact that part of the dynamics of the system is lost in the process of truncation (degeneration).

The main crux of the singular perturbation technique is to effectively utilize the simplicity offered by the order reduction and simultaneously recover the lost dynamics. To show the utility and effectiveness of this method for 2-D image model reduction, we need to put system (1) into a standard singularly perturbed form. To this end, let us define the following vertical state variables along the right-hand boundary by

$$x_i^v(m, n) = \epsilon^{M-N-i} y(m, n - M + i - 1),$$

$$\text{for } i \in [1, M - N - 1] \quad (4a)$$

and

$$x_i^v(m, n) = y(m, n - M + i - 1),$$

$$\text{for } i \in [M - N, M]. \quad (4b)$$

Propagating x_i^v's along the vertical direction gives

$$x_i^v(m, n + 1) = \epsilon\, x_{i+1}^v(m, n), \text{for } i \in [1, M - N - 1] \quad (5a)$$

and

$$x_i^v(m, n + 1) = x_{i+1}^v(m, n), \text{for } i \in [M - N, M - 1]. \quad (5b)$$

For x_M^v, we have

$$x_M^v(m, n + 1) = y(m, n)$$

$$= \sum_{q=1}^{N} a_{0,q} y(m, n - q)$$

$$+ \sum_{q=N+1}^{M} \epsilon^{q-N} a_{o,q} y(m, n - q)$$

$$+ x_1^h(m, n) + u(m, n) \quad (6a)$$

where

$$x_1^h(m, n) := \sum_{p=1}^{M} \sum_{q=0}^{M} \alpha_{p,q} y(m - p, n - q). \quad (6b)$$

The first and second terms in (6a) can be written in terms of x_i^v's as

$$x_M^v(m, n + 1) = \sum_{q=1}^{N} a_{0,q} x_{M-q+1}^v(m, n)$$
$$+ \sum_{q=N+1}^{M} \epsilon a_{0,q} x_{M-q+1}^v(m, n)$$
$$+ x_1^h(m, n) + u(m, n). \tag{7}$$

The horizontal state variable x_1^h can be propagated to give

$$x_1^h(m + 1, n) = \sum_{p=1}^{M} \sum_{q=0}^{M} \alpha_{p,q} y(m + 1 - p, n - q)$$
$$= a_{1,0} y(m, n) + \sum_{q=1}^{M} \alpha_{1,q} y(m, n - q)$$
$$+ x_2^h(m, n) \tag{8a}$$

where

$$x_2^h(m, n) := \sum_{p=2}^{M} \sum_{q=0}^{M} \alpha_{p,q} y(m + 1 - p, n - q). \tag{8b}$$

Replacing for $y(m, n)$ from (6a) yields

$$x_1^h(m + 1, n) = a_{1,0} x_1^h(m, n) + x_2^h(m, n)$$
$$+ \sum_{q=1}^{N-1} a_{1,q}^{(1)} x_{M-q+1}^v(m, n)$$
$$+ a_{1,N}^{(2)} x_{M-N+1}^v(m, n)$$
$$+ \epsilon \sum_{q=N+1}^{M} a_{1,q}^{(2)} x_{M-q+1}^v(m, n)$$
$$+ a_{1,0} u(m, n) \tag{9a}$$

where

$$a_{i,j}^{(k)} := a_{i,0} a_{0,j} + \epsilon^{k-1} a_{i,j}, \quad k = 1, 2, \cdots. \tag{9b}$$

A similar procedure can be applied to all x_i^h's, $i \in [2, N]$. The expression for $x_N^h(m + 1, n)$ is

$$x_N^h(m + 1, n) = \sum_{p=N}^{M} \sum_{q=0}^{M} \alpha_{p,q} y(m + N - p, n - q)$$
$$= a_{N,0} y(m, n) + \sum_{q=1}^{M} \epsilon^q a_{N,q} y(m, n - q)$$
$$+ \epsilon x_{N+1}^h(m, n) \tag{10a}$$

where

$$x_{N+1}^h(m, n) = \sum_{p=N+1}^{M} \sum_{q=0}^{M} (\alpha_{p,q}/\epsilon)$$
$$\cdot y(m + N - p, n - q). \tag{10b}$$

Again using (6a), we obtain

$$x_N^h(m + 1, n) = a_{N,0} x_1^h(m, n) + \epsilon x_{N+1}^h(m, n)$$
$$+ \sum_{q=1}^{N} a_{N,q}^{(q+1)} x_{M-q+1}^v(m, n)$$
$$+ \epsilon \sum_{q=N+1}^{M} a_{N,q}^{(N+1)} x_{M-q+1}^v(m, n)$$
$$+ a_{N,0} u(m, n). \tag{11a}$$

This process continues up to the last state variable, for which we get

$$x_M^h(m + 1, n) = a_{M,0} x_1^h(m, n)$$
$$+ \sum_{q=1}^{N} a_{M,q}^{(q+1)} x_{M-q+1}^v(m, n)$$
$$+ \epsilon \sum_{q=N+1}^{M} a_{M,q}^{(N+1)} x_{M-q+1}^v(m, n)$$
$$+ a_{M,0} u(m, n). \tag{11b}$$

Now, these equations can be arranged into the following 2-D local state-space model [11]:

$$\begin{bmatrix} \hat{X}^h(m + 1, n) \\ \hat{X}^v(m, n + 1) \end{bmatrix} = \begin{bmatrix} A_1 & A_2 \\ A_3 & A_4 \end{bmatrix} \begin{bmatrix} \hat{X}^h(m, n) \\ \hat{X}^v(m, n) \end{bmatrix}$$
$$+ \begin{bmatrix} B_1 \\ B_2 \end{bmatrix} u(m, n)$$
$$y(m, n) = \begin{bmatrix} C_1 & C_2 \end{bmatrix} \begin{bmatrix} \hat{X}^h(m, n) \\ \hat{X}^v(m, n) \end{bmatrix} + d u(m, n)$$
$$\tag{12}$$

where

$$\hat{X}^h(m, n) = \begin{bmatrix} \hat{X}^{hs}(m, n) \\ \hat{X}^{hf}(m, n) \end{bmatrix}, \hat{X}^v(m, n) = \begin{bmatrix} \hat{X}^{vs}(m, n) \\ \hat{X}^{vf}(m, n) \end{bmatrix}$$

$$\hat{X}^{hs} = \begin{bmatrix} x_1^h & \cdots & x_N^h \end{bmatrix}^t, \hat{X}^{hf} = \begin{bmatrix} x_{N+1}^h & \cdots & x_M^h \end{bmatrix}^t \tag{13a}$$

$$\hat{X}^{vs} = \begin{bmatrix} x_{M-N+1}^v & \cdots & x_M^v \end{bmatrix}^t$$

$$\hat{X}^{vf} = \begin{bmatrix} x_1^v & \cdots & x_{M-N}^v \end{bmatrix}^t \tag{13b}$$

and "t" denotes transposition.

The horizontal state $\hat{X}^h \in R^M$ is effectively partitioned into "slow" state, $\hat{X}^{hs} \in R^{n_s}$, $n_s = N$, and the "fast" state $\hat{X}^{hf} \in R^{n_f}$, $n_f = M - N$, corresponding to the strong and weak correlation areas, respectively. Similarly, the vertical state vector $\hat{X}^v \in R^M$ is partitioned into the "slow" state, $\hat{X}^{vs} \in R^{m_s}$, $m_s = N$, and the "fast" state $\hat{X}^{vf} \in R^{m_f}$, $m_f = M - N$, relating to the strong and weak correlation areas, respectively. Explicit definitions for fast/slow states are given

subsequently in Section III. The matrices in model (12) are defined as

$$A_1 = \begin{bmatrix} A_{11} & \epsilon A_{12} \\ A_{13} & \epsilon A_{14} \end{bmatrix}, A_2 = \begin{bmatrix} A_{21} & \epsilon A_{22} \\ A_{23} & \epsilon A_{24} \end{bmatrix} \quad (14a)$$

$$A_3 = \begin{bmatrix} A_{31} & \epsilon A_{32} \\ A_{33} & \epsilon A_{34} \end{bmatrix}, A_4 = \begin{bmatrix} A_{41} & \epsilon A_{42} \\ A_{43} & \epsilon A_{44} \end{bmatrix} \quad (14b)$$

$$B_1 = \begin{bmatrix} B_{11} \\ B_{12} \end{bmatrix}, B_2 = \begin{bmatrix} B_{21} \\ B_{22} \end{bmatrix} \quad (14c)$$

$$C_1 = \begin{bmatrix} C_{11} & \epsilon C_{12} \end{bmatrix}, C_2 = \begin{bmatrix} C_{21} & \epsilon C_{22} \end{bmatrix} \text{ and } d = 1 \quad (14d)$$

where

$$A_{11} = \begin{bmatrix} a_{10} & 1 & 0 & \cdots & 0 \\ a_{20} & 0 & 1 & \cdots & 0 \\ \cdot & & & & \\ a_{N-1,0} & 0 & & & 1 \\ a_{N,0} & 0 & \cdot & \cdots & 0 \end{bmatrix},$$

$$A_{12} = \begin{bmatrix} 0 & \cdot & \cdots & 0 \\ 0 & \cdot & \cdots & 0 \\ \vdots & & & \\ 1 & 0 & \cdots & 0 \end{bmatrix} \quad (15a)$$

$$A_{13} = \begin{bmatrix} a_{N+1,0} & 0 & \cdot & \cdots & 0 \\ a_{N+2,0} & 0 & \cdot & \cdots & 0 \\ \vdots & & & & \\ a_{M,0} & 0 & \cdot & \cdots & 0 \end{bmatrix},$$

$$A_{14} = \begin{bmatrix} 0 & 1 & \cdots & & 0 \\ 0 & 0 & 1 & \cdot & 0 \\ \cdot & & & & \\ \cdot & & & & 1 \\ 0 & 0 & \cdots & & 0 \end{bmatrix} \quad (15b)$$

$$A_{21} = \begin{bmatrix} a_{1,N}^{(2)} & a_{1,N-1}^{(1)} & \cdots & a_{1,1}^{(1)} \\ a_{2,N}^{(3)} & a_{2,N-1}^{(2)} & \cdots & a_{2,1}^{(1)} \\ \vdots & & & \vdots \\ a_{N,N}^{(N+1)} & a_{N,N-1}^{(N)} & \cdots & a_{N,1}^{(2)} \end{bmatrix},$$

$$A_{22} = \begin{bmatrix} a_{1,M}^{(2)} & a_{1,M-1}^{(2)} & \cdots & a_{1,N+1}^{(2)} \\ a_{2,M}^{(3)} & a_{2,M-1}^{(3)} & \cdots & a_{2,N+1}^{(3)} \\ \cdot & & & \\ a_{N,M}^{(N+1)} & a_{N,M-1}^{(N+1)} & \cdots & a_{N,N+1}^{(N+1)} \end{bmatrix} \quad (15c)$$

$$A_{23} = \begin{bmatrix} a_{N+1,N}^{(N+1)} & \cdots & a_{N+1,1}^{(2)} \\ a_{N+2,N}^{(N+1)} & \cdots & a_{N+2,1}^{(2)} \\ \vdots & & \\ a_{M,N}^{(N+1)} & \cdots & a_{M,1}^{(2)} \end{bmatrix},$$

$$A_{24} = \begin{bmatrix} a_{N+1,M}^{(N+1)} & \cdots & a_{N+1,N+1}^{(N+1)} \\ a_{N+2,M}^{(N+1)} & \cdots & a_{N+2,N+1}^{(N+1)} \\ \vdots & & \\ a_{M,M}^{(N+1)} & \cdots & a_{M,N+1}^{(N+1)} \end{bmatrix} \quad (15d)$$

$$A_{31} = \begin{bmatrix} 0 & \cdots & 0 \\ 0 & \cdots & 0 \\ 1 & & 0 \end{bmatrix}, A_{32} = \mathbf{0}, A_{33} = \mathbf{0}, A_{34} = \mathbf{0} \quad (15e)$$

$$A_{41} = \begin{bmatrix} 0 & 1 & & \cdots & 0 \\ 0 & 0 & & \cdots & 0 \\ \cdot & & & \cdot & \\ 0 & & & & 1 \\ a_{0,N} & a_{0,N-1} & & & a_{0,1} \end{bmatrix},$$

$$A_{42} = \begin{bmatrix} 0 & \cdots & \cdot & 0 \\ 0 & \cdots & \cdot & 0 \\ \vdots & & & \\ a_{0,M} & \cdots & & a_{0,N+1} \end{bmatrix} \quad (15f)$$

$$A_{43} = \begin{bmatrix} 0 & 0 & \cdots & 0 \\ 0 & 0 & \cdots & 0 \\ \vdots & & & \\ 1 & 0 & \cdots & 0 \end{bmatrix},$$

$$A_{44} = \begin{bmatrix} 0 & 1 & \cdots & 0 \\ 0 & 0 & 1 & 0 \\ & & \cdot & \\ & & & 1 \\ 0 & 0 & 0 & 0 \end{bmatrix} \quad (15g)$$

$$B_{11} = \begin{bmatrix} a_{1,0} \\ a_{2,0} \\ \vdots \\ a_{N,0} \end{bmatrix}, B_{12} = \begin{bmatrix} a_{N+1,0} \\ a_{N+2,0} \\ \vdots \\ a_{M,0} \end{bmatrix}, B_{21} = \begin{bmatrix} 0 \\ \cdot \\ \cdot \\ 1 \end{bmatrix}, B_{22} = \begin{bmatrix} 0 \\ 0 \\ \vdots \\ 0 \end{bmatrix} \quad (15h)$$

$$C_{11} = \begin{bmatrix} 1 \cdots 0 \end{bmatrix}, C_{12} = \begin{bmatrix} 0 \cdots 0 \end{bmatrix}$$

$$C_{21} = \begin{bmatrix} a_{0,N} & \cdots & a_{0,1} \end{bmatrix}, \text{ and } C_{22} = \begin{bmatrix} a_{0,M} & \cdots & a_{0,N+1} \end{bmatrix}. \quad (15i)$$

The 2-D state-space model (12) is now in singularly perturbed form. By setting the singular perturbation parameter ϵ to zero, the effects of weakly coupled pixels in region W_2 are totally ignored and as a consequence the order of the model (12) reduces from $M \times M$ for the entire region W to $N \times N$ corresponding to region W_1. However, this reduced-order system does not usually capture the essential characteristics of the full-order model (12). In the following sections a decomposition–aggregation strategy is introduced for 2-D singularly perturbed systems, which provides a tool for obtaining reduced-order 2-D subsystems that closely capture the dynamics of the original 2-D full-order system.

III. FAST–SLOW DECOMPOSITION IN 2-D STATE-SPACE MODELS

The first step in the process of model reduction using the singular perturbation scheme is to decompose the eigenvalues of matrices A_1 and A_4 into fast–slow parts. That is, given

the 2-D system (12), a similarity transformation is applied to the system such that matrices A_1 and A_4 are block diagonalized. Through this procedure the inherent dynamic separation becomes more evident.

Definition 3.1: Given the matrix A_1 (or A_4) corresponding to the horizontal (or vertical) state, an eigenvalue is defined as "slow/fast" if its magnitude is close to the boundary/origin of the unit circle (see also [1] for similar definitions). ∎

Definition 3.2: The horizontal (or vertical) state associated with the "slow/fast" dynamics is referred to as "slow/fast" state (see also [1]). ∎

The clustering in eigenvalues of A_1 and A_4 matrices is caused owing to the strong-weak coupling effects in the ROS of the image model. The slow eigenvalues of A_1 and A_4 correspond to the strongly coupled states while the fast eigenvalues are associated with the weakly coupled states. Now, let us assume that the eigenvalues are clustered into two distinct sets of n_s and n_f for matrix A_1 and m_s and m_f for matrix A_4 such that

  i) $n_s + n_f = M$,
  ii) $m_s + m_f = M$,
  iii) denote $\lambda_s := \min |\lambda_i(A_1)|$, $i \in [1, n_s]$ and $\lambda_f := \max |\lambda_j(A_1)|$, $j \in [1, n_f]$, then $\lambda_f \ll \lambda_s$, and
  iv) denote $\lambda'_s := \min |\lambda_i(A_4)|$, $i \in [1, m_s]$ and $\lambda'_f := \max |\lambda_j(A_4)|$, $j \in [1, m_f]$, then $\lambda'_f \ll \lambda'_s$.

Under the above conditions there will exist bases in R^M such that both matrices A_1 and A_4 are block diagonalizable. This is discussed in the following lemma derived from the results in [12].

Lemma 3.1: Assuming that the eigenvalue clustering conditions above are satisfied, similarity transformation matrices of the form

$$T_1 = \begin{bmatrix} I_{n_s} - M_1 L_1 & -M_1 \\ L_1 & I_{n_f} \end{bmatrix}, \quad T_2 = \begin{bmatrix} I_{m_s} - M_2 L_2 & -M_2 \\ L_2 & I_{m_f} \end{bmatrix} \tag{16}$$

exist, which block diagonalize matrices A_1 and A_4, respectively, such that

$$T_1 A_1 T_1^{-1} = \begin{bmatrix} A_1^s & 0 \\ 0 & A_1^f \end{bmatrix}, \quad T_2 A_4 T_2^{-1} = \begin{bmatrix} A_4^s & 0 \\ 0 & A_4^f \end{bmatrix} \tag{17a}$$

where

$$A_1^s := A_{11} - \epsilon A_{12} L_1, \quad A_4^s := A_{41} - \epsilon A_{42} L_2 \tag{17b}$$

$$A_1^f := \epsilon(A_{14} + L_1 A_{12}), \quad A_4^f := \epsilon(A_{44} + L_2 A_{42}) \tag{17c}$$

and I_{n_s}, I_{n_f}, I_{m_s}, and I_{m_f} are identity matrices of dimension n_s, n_f, m_s, and m_f, respectively. Matrices L_1, M_1 and L_2, M_2 satisfy the following Riccati and Lyapunov type equations:

$$L_1 A_{11} - \epsilon A_{14} L_1 - \epsilon L_1 A_{12} L_1 + A_{13} = 0 \tag{18a}$$

$$A_{11} M_1 - \epsilon A_{12} L_1 M_1 + \epsilon A_{12}$$
$$- \epsilon M_1 L_1 A_{12} - \epsilon M_1 A_{14} = 0 \tag{18b}$$

and

$$L_2 A_{41} - \epsilon A_{44} L_2 - \epsilon L_2 A_{42} L_2 + A_{43} = 0 \tag{19a}$$

$$A_{41} M_2 + \epsilon A_{42} - \epsilon M_2 L_2 A_{42}$$
$$- \epsilon M_2 A_{44} - \epsilon A_{42} L_2 M_2 = 0. \tag{19b}$$
∎

Remark 3.1: The "zeroth-order" approximation for L_1, M_1 and L_2, M_2 are obtained for $\epsilon = 0$ as

$$L_1^{(0)} = -A_{13} A_{11}^{-1} \text{ and } M_1^{(0)} = 0$$

$$L_2^{(0)} = -A_{43} A_{41}^{-1} \text{ and } M_2^{(0)} = 0 \tag{20}$$

where it is assumed that A_{11}^{-1} and A_{41}^{-1} exist (this is a necessary condition for dynamic separation property [12]). The contraction mapping argument of [12] can be used to develop a computationally efficient iterative procedure to evaluate, for a sufficiently small ϵ, L_1, M_1 and L_2, M_2 as follows:

$$L_1^{(k)} = \left(\epsilon A_{14} L_1^{(k-1)} + \epsilon L_1^{(k-1)} A_{12} L_1^{(k-1)} - A_{13} \right) A_{11}^{-1} \tag{21a}$$

$$M_1^{(k)} = \epsilon A_{11}^{-1} \left[A_{12} L_1^{(k-1)} M_1^{(k-1)} + M_1^{(k-1)} \left(A_{14} + L_1^{(k-1)} A_{12} \right) - A_{12} \right] \tag{21b}$$

and

$$L_2^{(k)} = \left(\epsilon A_{44} L_2^{(k-1)} + \epsilon L_2^{(k-1)} A_{42} L_2^{(k-1)} - A_{43} \right) A_{41}^{-1} \tag{22a}$$

$$M_2^{(k)} = \epsilon A_{41}^{-1} \left[A_{42} L_2^{(k-1)} M_2^{(k-1)} + M_2^{(k-1)} \left(A_{44} + L_2^{(k-1)} A_{42} \right) - A_{42} \right]. \tag{22b}$$

It is clearly seen that M_1 and M_2 are $0(\epsilon)$ matrices whereas L_1 and L_2 are $0(1)$ matrices. ∎

Now, following the results developed in [12] and [13], sufficiency conditions for the existence and uniqueness of real solutions for L_1 and L_2 and bounds on ϵ may be obtained. The result is summarized in the following lemma.

Lemma 3.2: A unique solution to (18a) and (19a) exists if A_{11} and A_{41} are nonsingular and ϵ is within the bounds defined by $0 \leq \epsilon \leq \hat{\epsilon} = \min(\hat{\epsilon}_1, \hat{\epsilon}_2)$, where $\|A\| = [\lambda_{\max}(A^*A)]^{1/2}$, $* \triangleq$ conjugate transpose with

$$0 \leq \hat{\epsilon}_1 < \frac{1}{3\|A_{11}^{-1}\|(\|A_{14} + L_1^{(0)} A_{12}\| + \|A_{12}\| \|L_1^{(0)}\|)} \tag{23a}$$

and

$$0 \leq \hat{\epsilon}_2 < \frac{1}{3\|A_{41}^{-1}\|(\|A_{44} + L_2^{(0)} A_{42}\| + \|A_{42}\| \|L_2^{(0)}\|)}. \tag{23b}$$

Proof: Follows immediately from the results in [12]. ∎
By expressing (18b) as

$$(A_{11} - \epsilon A_{12} L_1) M_1 - \epsilon M_1 (A_{14} + L_1 A_{12}) + \epsilon A_{12} = 0 \tag{24a}$$

or alternatively

$$A_1^s M_1 - M_1 A_1^f + \epsilon A_{12} = 0 \qquad (24b)$$

and similarly for (19b),

$$A_4^s M_2 - M_2 A_4^f + \epsilon A_{42} = 0 \qquad (25)$$

it is well known that the Lyapunov type equations (24) and (25) have unique solutions, since A_1^s and A_1^f, and A_4^s and A_4^f, have no eigenvalues in common. Therefore, the above bound on ϵ provides a sufficient condition for block diagonalization and dynamic separation of the original system (12). With the dynamic separation property satisfied, the eigenvalues of A_1 are now partitioned into the slow and fast eigenvalues associated with those of A_1^s and A_1^f, respectively; and similarly the eigenvalues of A_4 are partitioned into the slow and fast eigenvalues associated with those of A_4^s and A_4^f, respectively. The eigenvalues of A_1 can be ordered as $\lambda_M \leq \lambda_{M-1} \leq \cdots \leq \lambda_{M-n_f+1} \ll \lambda_{M-n_f} \leq \cdots \leq \lambda_1$, with n_s and n_f denoting the number of slow and fast eigenvalues of A_1, respectively, and the eigenvalues of A_4 can be ordered as $\lambda'_M \leq \lambda'_{M-1} \leq \cdots \leq \lambda'_{M-m_f+1} \ll \lambda'_{M-m_f} \leq \cdots \leq \lambda'_1$, with m_s and m_f denoting the number of slow and fast eigenvalues of A_4, respectively. Thus the similarity transformation matrix T_1 partitions the eigenvalues of A_1 into the slow and fast eigenvalues of A_1^s and A_1^f, respectively, and the similarly transformation matrix T_2 partitions the eigenvalues of A_4 into the slow and fast eigenvalues of A_4^s and A_4^f, respectively. Note that the perturbation parameter ϵ can be interpreted as representing a gap between the largest of the fast eigenvalues and the smallest of the slow eigenvalues. The ratio between these two eigenvalues has been used in practice [13] for quantifying ϵ. For the 2-D case we can use

$$\epsilon_1 = |\lambda_{M-n_f+1}| / |\lambda_{M-n_f}| \text{ or}$$

$$\epsilon_1 = |1 - \lambda_{M-n_f}| / |1 - \lambda_{M-n_f+1}| \qquad (26)$$

and

$$\epsilon_2 = |\lambda'_{M-m_f+1}| / |\lambda'_{M-m_f}| \text{ or}$$

$$\epsilon_2 = |1 - \lambda'_{M-m_f}| / |1 - \lambda'_{M-m_f+1}|. \qquad (27)$$

Then set $\epsilon := \text{Max } (\epsilon_1, \epsilon_2)$. Note that the estimates given by (23a) and (23b) would guarantee the existence of a convergent solution to the Riccati-type equations. This is to be distinguished from the perturbation parameter used in (2), or equivalently defined in (26) and (27). To clarify this point, if we are given only state equation (12) without an explicit definition of ϵ, then we would use equations (26) and (27) to define ϵ as the gap between the fast and slow eigenvalues. This happens to be the situation we have for the two numerical examples in Section VI. Once ϵ is defined this way, we then check (23a, b) to ensure that solutions to the Riccati-type equations do exist. In the numerical examples in Section VI, the exact solutions have actually been obtained in a few iterations, which suggests that conditions (23a) and (b) are indeed satisfied. We can now state the main result of this section in the following lemma.

Lemma 3.3: A similarity transformation matrix $T = T_1 \oplus T_2$ exists, with $\oplus$ denoting the direct sum operation, and the new transformed 2-D state vector defined by

$$\begin{bmatrix} X^h(m, n) \\ X^v(m, n) \end{bmatrix} = \begin{bmatrix} T_1 & 0 \\ 0 & T_2 \end{bmatrix} \begin{bmatrix} \hat{X}^h(m, n) \\ \hat{X}^v(m, n) \end{bmatrix} \qquad (28)$$

such that the transformed state and output equations are

$$\begin{bmatrix} X^h(m + 1, n) \\ X^v(m, n + 1) \end{bmatrix} = \begin{bmatrix} T_1 A_1 T_1^{-1} & T_1 A_2 T_2^{-1} \\ T_2 A_3 T_1^{-1} & T_2 A_4 T_2^{-1} \end{bmatrix}$$
$$\cdot \begin{bmatrix} X^h(m, n) \\ X^v(m, n) \end{bmatrix} + \begin{bmatrix} T_1 B_1 \\ T_2 B_2 \end{bmatrix} u(m, n) \qquad (29a)$$

$$y(m, n) = \begin{bmatrix} C_1 T_1^{-1} & C_2 T_2^{-1} \end{bmatrix} \begin{bmatrix} X^h(m, n) \\ X^v(m, n) \end{bmatrix} + d u(m, n). \qquad (29b)$$

If T_1 and T_2 are chosen as in Lemma 3.1, the transformed 2-D state-space equations are

$$\begin{bmatrix} X^{hs}(m + 1, n) \\ X^{hf}(m + 1, n) \\ \hline X^{vs}(m, n + 1) \\ X^{vf}(m, n + 1) \end{bmatrix} = \begin{bmatrix} A_1^s & 0 & B_{11}^s & \epsilon B_{12}^f \\ 0 & A_1^f & B_{13}^s & \epsilon B_{14}^f \\ \hline C_{11}^s & \epsilon C_{12}^f & A_4^s & 0 \\ C_{13}^s & \epsilon C_{14}^f & 0 & A_4^f \end{bmatrix}$$
$$\cdot \begin{bmatrix} X^{hs}(m, n) \\ X^{hf}(m, n) \\ \hline X^{vs}(m, n) \\ X^{vf}(m, n) \end{bmatrix} + \begin{bmatrix} D_{11}^s \\ D_{12}^f \\ \hline D_{13}^s \\ D_{14}^f \end{bmatrix} u(m, n)$$

$$(30a)$$

$$y(m, n) = \begin{bmatrix} E_{11}^s E_{12}^f & E_{13}^s E_{14}^f \end{bmatrix} \begin{bmatrix} X^{hs}(m, n) \\ X^{hf}(m, n) \\ \hline X^{vs}(m, n) \\ X^{vf}(m, n) \end{bmatrix}$$
$$+ d u(m, n) \qquad (30b)$$

where

$$X^h(m, n) = \begin{bmatrix} X^{hs}(m, n) \\ X^{hf}(m, n) \end{bmatrix}, \quad X^v(m, n) = \begin{bmatrix} X^{vs}(m, n) \\ X^{vf}(m, n) \end{bmatrix},$$

with $X^{hs} \in R^{n_s}$, $X^{hf} \in R^{n_f}$, $X^{vs} \in R^{m_s}$, and $X^{vf} \in R^{m_f}$; and

$$T_1 A_2 T_2^{-1} := \begin{bmatrix} B_{11}^s & \epsilon B_{12}^f \\ B_{13}^s & \epsilon B_{14}^f \end{bmatrix}, T_2 A_3 T_1^{-1} := \begin{bmatrix} C_{11}^s & \epsilon C_{12}^f \\ C_{13}^s & \epsilon C_{14}^f \end{bmatrix}$$

$$T_1 B_1 := \begin{bmatrix} D_{11}^s \\ D_{12}^f \end{bmatrix}, T_2 B_2 := \begin{bmatrix} D_{13}^s \\ D_{14}^f \end{bmatrix},$$

$$C_1 T_1^{-1} := \begin{bmatrix} E_{11}^s E_{12}^f \end{bmatrix}, C_2 T_2^{-1} := \begin{bmatrix} E_{13}^s E_{14}^f \end{bmatrix} \qquad (31)$$

and

$$A_1^s = A_{11} - \epsilon A_{12} L_1$$

$$B_{11}^s = (A_{21} - M_1 A_{23} - M_1 L_1 A_{21})$$
$$+ \epsilon(M_1 A_{24} + M_1 L_1 A_{22} - A_{22}) L_2$$

$$\epsilon B_{12}^f = \epsilon(A_{22} - M_1 L_1 A_{22} - M_1 A_{24}) + B_{11}^s M_2$$

$$A_1^f = \epsilon(A_{14} + L_1 A_{12})$$

$$B_{13}^s = (A_{23} + L_1 A_{21}) - \epsilon(A_{24} + L_1 A_{22}) L_2$$

$$\epsilon B_{14}^f = \epsilon(A_{24} + L_1 A_{22}) + B_{13}^s M_2$$

$$C_{11}^s = (A_{31} - M_2 A_{33} - M_2 L_2 A_{31})$$
$$+ \epsilon(-A_{32} + M_2 A_{34} + M_2 L_2 A_{32}) L_1$$

$$\epsilon C_{12}^f = \epsilon(A_{32} - M_2 L_2 A_{32} - M_2 A_{34}) + C_{11}^s M_1$$

$$A_4^s = A_{41} - \epsilon A_{42} L_2$$

$$C_{13}^s = (A_{33} + L_2 A_{31}) - \epsilon(L_2 A_{32} + A_{34}) L_1$$

$$\epsilon C_{14}^f = \epsilon(A_{34} + L_2 A_{32}) + C_{13}^s M_1$$

$$A_4^f = \epsilon(A_{44} + L_2 A_{42})$$

$$D_{11}^s = (I - M_1 L_1) B_{11} - M_1 B_{12}$$

$$D_{12}^f = B_{12} + L_1 B_{11}, \quad D_{13}^s = (I - M_2 L_2) B_{21} - M_2 B_{22}$$

$$D_{14}^f = B_{22} + L_2 B_{21}$$

$$E_{11}^s = C_{11} - \epsilon C_{12} L_1, \quad E_{12}^f = \epsilon C_{12} + C_{11} M_1 - \epsilon C_{12} L_1 M_1$$

$$E_{13}^s = C_{21} - \epsilon C_{22} L_2 - \epsilon C_{22} L_2 M_2$$

$$E_{14}^f = \epsilon C_{22} + C_{21} M_2. \tag{32}$$

Proof: The proof follows from the results obtained in [9] and [10]. Note that in Remark 3.1 it was pointed out that M_1 and M_2 are $O(\epsilon)$ matrices. Thus the terms $B_{11}^s M_2$, $B_{13}^s M_1$, $C_{11}^s M_1$, and $C_{13}^s M_2$ are $O(\epsilon)$ matrices implying that ϵB_{12}^f, ϵB_{14}^f, ϵC_{12}^f, and ϵC_{14}^f are also $O(\epsilon)$ matrices. ∎

So far the eigenvalues of matrices A_1 and A_4 are decomposed into the fast and the slow eigenvalues via the application of the block diagonalizing transformations T_1 and T_2 in (16). In contrast to the 1-D case [12], where the block diagonalizing transformation would lead to an exact dynamic separation and hence an exact model reduction, in the 2-D case these transformations by themselves would not result in a dynamic separation or model reduction as evident from the state matrix in system (30). Nonetheless, these transformations result in dynamic separation along each direction independently, i.e., the dynamics along the horizontal and vertical directions alone are separated as evident from the upper left and lower right blocks in the state matrix of system (30). In the next section a method is introduced that can be used to effectively reduce the general transformed 2-D system (30) into two reduced-order 2-D subsystems associated with slow and fast dynamics.

IV. MODEL REDUCTION AND AGGREGATION FOR SINGULARLY PERTURBED 2-D SYSTEMS

A singularly perturbed system exhibits, in general, a multitime-scale behavior characterized by the presence of both slow and fast dynamics in the system response. The slow response of system (30) contains contributions from both the fast variables as well as the slow variables. Similarly, the fast response of system (30) contains contributions from both the fast variables as well as the slow variables. The fast variables themselves contain a pure fast part that characterizes the "fast transient" and a slow part, which is referred to as the "quasi-steady-state" (see Definition 4.1). In order to accomplish dynamic separation and subsequently model reduction without losing the effects of the corresponding fast dynamics in the reduced-order slow subsystem, the effects of the quasi-steady-states are incorporated into the slow dynamics. This is achieved by defining new fast variables that represent the pure fast variables (or fast transients) by removing the quasi-steady-state parts from the fast variables and then aggregating these quasi-steady-state parts into the slow variables. Interestingly enough, if the dynamics of the pure fast subsystem is asymptotically stable the effect of the fast transients on the slow subsystem would vanish quickly. This can be seen from the numerical examples in Section V. Note that the difference between the response of the original full-order system with $\epsilon = 0$ and that of the slow subsystem is that the latter response has embedded in it the aggregated effects of the fast variables (the quasi-steady-state parts).

Let us first rearrange the 2-D full-order system (30) such that the slow horizontal and vertical states, and also the fast horizontal and vertical states, are grouped together. This yields

$$
\begin{bmatrix} X^{hs}(m+1,n) \\ X^{vs}(m,n+1) \\ X^{hf}(m+1,n) \\ X^{vf}(m,n+1) \end{bmatrix}
=
\begin{bmatrix} A_1^s & B_{11}^s & 0 & \epsilon B_{12}^f \\ C_{11}^s & A_4^s & \epsilon C_{12}^f & 0 \\ 0 & B_{13}^s & A_1^f & \epsilon B_{14}^f \\ C_{13}^s & 0 & \epsilon C_{14}^f & A_4^f \end{bmatrix}
$$
$$
\cdot
\begin{bmatrix} X^{hs}(m,n) \\ X^{vs}(m,n) \\ X^{hf}(m,n) \\ X^{vf}(m,n) \end{bmatrix}
+
\begin{bmatrix} D_{11}^s \\ D_{13}^s \\ D_{12}^f \\ D_{14}^f \end{bmatrix} u(m,n) \tag{33a}
$$

$$
y(m,n) = \begin{bmatrix} E_{11}^s & E_{13}^s & E_{12}^f & E_{14}^f \end{bmatrix}
$$
$$
\cdot
\begin{bmatrix} X^{hs}(m,n) \\ X^{vs}(m,n) \\ X^{hf}(m,n) \\ X^{vf}(m,n) \end{bmatrix}
+ d\,u(m,n). \tag{33b}
$$

As already discussed the aggregation is accomplished by replacing the original fast states with their new fast variables which simply represent the deviation of the fast states from their quasi-steady-state values. But let us first define the term "quasi-steady-state" properly.

Definition 4.1: The quasi-steady-states $\overline{X}^{hf}$ and $\overline{X}^{vf}$ are defined from the full-order system by allowing no propaga-

tion occurring in the horizontal and vertical directions in the fast states X^{hf} and X^{vf}, respectively. That is, the quasi-steady-states are defined under the condition that $\overline{X}^{hf}(m + 1, n) = \overline{X}^{hf}(m, n)$ and $\overline{X}^{vf}(m, n + 1) = \overline{X}^{vf}(m, n)$, which is equivalent to treating the fast states as being "frozen" in the appropriate directions. ∎

From the Definition 4.1 of the quasi-steady-states $\overline{X}^{hf}$ and $\overline{X}^{vf}$ one gets

$$\overline{X}^{hf}(m, n) = B_{13}^s X^{vs}(m, n) + A_1^f \overline{X}^{hf}(m, n)$$
$$+ \epsilon B_{14}^f \overline{X}^{vf}(m, n) + D_{12}^f u(m, n) \quad (34a)$$

$$\overline{X}^{vf}(m, n) = C_{13}^s X^{hs}(m, n) + A_4^f \overline{X}^{vf}(m, n)$$
$$+ \epsilon C_{14}^f \overline{X}^{hf}(m, n) + D_{14}^f u(m, n). \quad (34b)$$

Now, using (34a) and (b), the quasi-steady-states $\overline{X}^{hf}$ and $\overline{X}^{vf}$ of the fast variables may be expressed in terms of the slow states and the input by

$$\overline{X}^{hf}(m, n) = \mathbf{K}_1 X^{vs}(m, n) + \mathbf{K}_2 X^{hs}(m, n)$$
$$+ D_1 u(m, n) \quad (35a)$$

$$\overline{X}^{vf}(m, n) = \mathbf{K}_3 X^{vs}(m, n) + \mathbf{K}_4 X^{hs}(m, n)$$
$$+ D_2 u(m, n) \quad (35b)$$

where

$$\mathbf{K}_1 := (I - R_2 R_4)^{-1} R_1, \mathbf{K}_2 := (I - R_2 R_4)^{-1} R_2 R_3$$

$$\mathbf{K}_3 := (I - R_4 R_2)^{-1} R_4 R_1, \mathbf{K}_4 := (I - R_4 R_2)^{-1} R_3$$

and

$$D_1 := (I - R_2 R_4)^{-1} (R_2 S_2 + S_1)$$
$$D_2 := (I - R_4 R_2)^{-1} (R_4 S_1 + S_2) \quad (36a)$$

with

$$R_1 := (I - A_1^f)^{-1} B_{13}^s, \ R_2 := \epsilon (I - A_1^f)^{-1} B_{14}^f$$

$$R_3 := (I - A_4^f)^{-1} C_{13}^s, \ R_4 := \epsilon (I - A_4^f)^{-1} C_{14}^f$$

$$S_1 := (I - A_1^f)^{-1} D_{12}^f, \text{ and } S_2 := (I - A_4^f)^{-1} D_{14}^f. \quad (36b)$$

In contrast to the original fast variables which could initially, say at $m = m_o$ and $n = n_o$, take arbitrary values $X^{hf}(m_o, n_o)$ and $X^{vf}(m_o, n_o)$, the quasi-steady-states are not free to start from $X^{hf}(m_o, n_o)$ and $X^{vf}(m_o, n_o)$. As a matter of fact, (35) constrains the initial values of the quasi-steady-states at

$$\overline{X}^{hf}(m_o, n_o) = \mathbf{K}_1 X^{vs}(m_o, n_o) + \mathbf{K}_2 X^{hs}(m_o, n_o)$$
$$+ D_1 u(m_o, n_o)$$

$$\overline{X}^{vf}(m_o, n_o) = \mathbf{K}_3 X^{vs}(m_o, n_o) + \mathbf{K}_4 X^{hs}(m_o, n_o)$$
$$+ D_2 u(m_o, n_o)$$

which could, in general, be far from $X^{hf}(m_o, n_o)$ and $X^{vf}(m_o, n_o)$. Therefore, (35) cannot be a uniform approximation of the fast states. Strictly speaking, we can only approximate the fast variables by their quasi-steady-states on an interval $(m, n) \in [(m_1, n_1), (m_t, n_t)]$ where $(m_1, n_1) \gg$

(m_o, n_o), by $X^{hf}(m, n) \cong \overline{X}^{hf}(m, n)$ and $X^{vf}(m, n) \cong \overline{X}^{vf}(m, n)$. Consequently, from the initial values at (m_o, n_o), the fast variables may deviate significantly from their quasi-steady-states up to (m_1, n_1), during which the original fast variables approach their quasi-steady-states values and then, during $[(m_1, n_1), (m_t, n_t)]$ remain close to quasi-steady-state values. We can now introduce new pure fast variables that represent the deviation of the fast variables X^{hf} and X^{vf} from their quasi-steady-states, as

$$Z^{hf}(m, n) = X^{hf}(m, n) - \overline{X}^{hf}(m, n) \quad (38a)$$

$$Z^{vf}(m, n) = X^{vf}(m, n) - \overline{X}^{vf}(m, n). \quad (38b)$$

It is a standard procedure in the singular perturbation literature to express the slow subsystem in the "slow-time-scale" and the fast subsystem in the "fast-time-scale" [14]. Here we have kept the work "time" for the sake of conformity with literature, although strictly speaking due to the nature of 2-D systems the word "space" would have been more appropriate. The system (12), and (30), are both expressed in the slow-time-scale. To construct the fast subsystem we need to define a fast-time-scale. This is done by relating the slow-time-scale m and n to the fast-time-scale k and l [14] using

$$k = m[1/\epsilon], \text{ and } l = n[1/\epsilon] \quad (39)$$

where $[1/\epsilon]$ is the largest integer $\leq 1/\epsilon$. We assume that the input is slowly time varying in the slow-time-scale, so that we have $u(k + 1, l) = u(k, l)$ and $u(k, l + 1) = u(k, l)$ in the fast-time-scale. Furthermore, we assume that the slow variables X^{hs} and X^{vs} remain constant during the fast transients in the fast-time-scale, which implies that $\overline{X}^{hf}(k + 1, l) = \overline{X}^{hf}(k, l)$ and $\overline{X}^{vf}(k, l + 1) = \overline{X}^{vf}(k, l)$ (since they contain only slow variables). We are now in a position to obtain the fast subsystem.

The dynamics of the new pure fast variables Z^{hf} and Z^{vf} are specified from (38) in the fast-time-scale by

$$Z^{hf}(k + 1, l) = X^{hf}(k + 1, l) - \overline{X}^{hf}(k + 1, l) \quad (40a)$$

$$Z^{vf}(k, l + 1) = X^{vf}(k, l + 1) - \overline{X}^{vf}(k, l + 1). \quad (40b)$$

Using (33) and (38) we have

$$Z^{hf}(k + 1, l) = B_{13}^s X^{vs}(k, l) + A_1^f \overline{X}^{hf}(k, l)$$
$$+ A_1^f Z^{hf}(k, l) + \epsilon B_{14}^f \overline{X}^{vf}(k, l)$$
$$+ \epsilon B_{14}^f Z^{vf}(k, l)$$
$$+ D_{12}^f u(k, l) - \overline{X}^{hf}(k, l) \quad (41a)$$

and

$$Z^{vf}(k, l + 1) = C_{13}^s X^{hs}(k, l) + A_4^f \overline{X}^{vf}(k, l)$$
$$+ A_4^f Z^{vf}(k, l) + \epsilon C_{14}^f \overline{X}^{hf}(k, l)$$
$$+ \epsilon C_{14}^f Z^{hf}(k, l)$$
$$+ D_{14}^f u(k, l) - \overline{X}^{vf}(k, l). \quad (41b)$$

Now, using (34a) and (b), Equations (41a) and (b) yield the fast subsystem given by

$$Z^{hf}(k+1, l) = A_1^f Z^{hf}(k, l) + \epsilon B_{14}^f Z^{vf}(k, l) \quad (42a)$$

$$Z^{vf}(k, l+1) = A_4^f Z^{vf}(k, l) + \epsilon C_{14}^f Z^{hf}(k, l). \quad (42b)$$

The solution of $Z^{hf}(k, l)$ and $Z^{vf}(k, l)$ from the fast subsystem may now be used as a correction to the quasi-steady-states $\overline{X}^{hf}$ and $\overline{X}^{vf}$ for a uniform approximation of X^{hf} and X^{vf}. The application of change of the fast variables using (38), which represent translations in these states, results in the aggregated full-order system. The result is presented in the following lemma.

Lemma 4.1: Under the assumption of the slow time-varying of the input, and that the slow variables remain constant during the fast transients in the fast-time-scale, the complete aggregated state equations for the full-order system (33) in terms of the new fast variables can be expressed as

$$X^{hs}(m+1, n) = \overline{A}_1^s X^{hs}(m, n) + \overline{B}_{11}^s X^{vs}(m, n)$$
$$+ \epsilon B_{12}^f Z^{vf}(m, n) + \overline{D}_1^s u(m, n)$$

$$X^{vs}(m, n+1) = \overline{C}_{11}^s X^{hs}(m, n) + \overline{A}_4^s X^{vs}(m, n)$$
$$+ \epsilon C_{12}^f Z^{hf}(m, n) + \overline{D}_2^s u(m, n)$$

$$Z^{kf}(k+1, l) = A_1^f Z^{hf}(k, l) + \epsilon B_{14}^f Z^{vf}(k, l)$$

$$Z^{vf}(k, l+1) = \epsilon C_{14}^f Z^{hf}(k, l) + A_4^f Z^{vf}(k, l)$$

$$y(m, n) = \overline{E}_1^s X^{hs}(m, n) + \overline{E}_2^s X^{vs}(m, n)$$
$$+ E_{12}^f Z^{hf}(m[1/\epsilon], n[1/\epsilon])$$
$$+ E_{14}^f Z^{vf}(m[1/\epsilon], n[1/\epsilon])$$
$$+ \overline{d}u(m, n) \quad (43)$$

where

$$\overline{A}_1^s := A_1^s + \epsilon B_{12}^f \mathbf{K}_4, \quad \overline{B}_{11}^s := B_{11}^s + \epsilon B_{12}^f \mathbf{K}_3$$

$$\overline{A}_4^s := A_4^s + \epsilon C_{12}^f \mathbf{K}_1, \quad \overline{C}_{11}^s := C_{11}^s + \epsilon C_{12}^f \mathbf{K}_2$$

$$\overline{D}_1^s := D_{11}^s + \epsilon B_{12}^f D_2, \quad \overline{D}_2^s := D_{13}^s + \epsilon C_{12}^f D_1.$$

$$\overline{E}_1^s := E_{11}^s + E_{12}^f \mathbf{K}_2 + E_{14}^f \mathbf{K}_4, \quad \overline{E}_2^s := E_{13}^s + E_{12}^f \mathbf{K}_1 + E_{14}^f \mathbf{K}_3$$

$$\overline{d} := E_{12}^f D_1 + E_{14}^f D_2 + d. \quad (44)$$

Proof: The proof follows along the results outlined above (also see [7] and [8] for more details). ∎

As can be seen from (43), the slow part of state is now dependent on the prior slow states and the pure prior fast states. The fast part of state is not externally excited and since the eigenvalues of A_1^f and A_4^f matrices are located in a cluster close to the origin of the unit circle, the fast dynamics decay quickly. We are now in a position to define the reduced-order 2-D slow and fast subsystems.

2-D Slow Subsystem: The reduced-order 2-D slow subsystem is obtained by neglecting the $0(\epsilon)$ fast terms $\epsilon B_{12}^f Z^{vf}$ and $\epsilon C_{12}^f Z^{hf}$ in (43) (representing the weak external interconnections between slow and fast subsystems). This subsystem, which represents the dominant part of the response and

captures the dynamics of the strongly correlated pixels, is given by

$$\begin{bmatrix} \tilde{X}^{hs}(m+1, n) \\ \tilde{X}^{vs}(m, n+1) \end{bmatrix} = \begin{bmatrix} \overline{A}_1^s & \overline{B}_{11}^s \\ \overline{C}_{11}^s & \overline{A}_4^s \end{bmatrix} \begin{bmatrix} \tilde{X}^{hs}(m, n) \\ \tilde{X}^{vs}(m, n) \end{bmatrix}$$
$$+ \begin{bmatrix} \overline{D}_1^s \\ \overline{D}_2^s \end{bmatrix} u(m, n) \quad (45a)$$

$$y^s(m, n) = \overline{E}_1^s \tilde{X}^{hs}(m, n) + \overline{E}_2^s \tilde{X}^{vs}(m, n)$$
$$+ \overline{d}u(m, n) \quad (45b)$$

where the notation $\tilde{X}^{hs}$ and $\tilde{X}^{vs}$ are used instead of X^{hs} and X^{vs} to distinguish the response of (45) from that of (43). The discrepancy between the full-order model (33) and the reduced-order slow subsystem (45) is characterized by the fast subsystem obtained from (43) as the following.

2-D Fast Subsystem: The fast subsystem which has captured the dynamics of the weakly correlated pixels is

$$\begin{bmatrix} Z^{hf}(k+1, l) \\ Z^{vf}(k, l+1) \end{bmatrix} = \begin{bmatrix} A_1^f & \epsilon B_{14}^f \\ \epsilon C_{14}^f & A_4^f \end{bmatrix} \begin{bmatrix} Z^{hf}(k, l) \\ Z^{vf}(k, l) \end{bmatrix} \quad (46a)$$

$$y^f(k, l) = E_{12}^f Z^{hf}(k, l) + E_{14}^f Z^{vf}(k, l). \quad (46b)$$

The terms $y^s(m, n)$ and $y^f(k, l)$ represent the slow subsystem and the fast subsystem outputs, respectively. The actual output of the 2-D system (33) is related to the slow and fast subsystem outputs by

$$y(m, n) = y^s(m, n) + y^f(m[1/\epsilon], n[1/\epsilon]) + 0(\epsilon). \quad (47)$$

Provided that there exists an $\overline{\epsilon} > 0$ such that for all $\epsilon \in [0, \overline{\epsilon}]$, the 2-D systems (45) and (46) are stable, then the solutions to the decoupled 2-D state equations (45) and (46) are related to the solutions of the full-order 2-D system (33) by the following expressions:

$$X^{hs}(m, n) = \tilde{X}^{hs}(m, n) + 0(\epsilon)$$

$$X^{vs}(m, n) = \tilde{X}^{vs}(m, n) + 0(\epsilon) \quad (48a)$$

$$X^{hf}(m, n) = \overline{X}^{hf}(m, n)$$
$$+ Z^{hf}(m[1/\epsilon], n[1/\epsilon]) + 0(\epsilon)$$

$$X^{vf}(m, n) = \overline{X}^{vf}(m, n)$$
$$+ Z^{vf}(m[1/\epsilon], n[1/\epsilon]) + 0(\epsilon). \quad (48b)$$

The reduction in the computational effort is now attainable as a direct consequence of reduction in the model dimensionality. The stability properties of the reduced-order models and their relations to those of the full-order model are established in [9] and [10].

V. IMPLEMENTATION AND RESULTS

5.1. Image Modeling Example

The model reduction scheme developed in the previous sections is examined on the Lena image in Fig. 2, which has a resolution of 512×512 and the number of gray levels which is 256. A third-order 2-D autoregressive (AR) model

Fig. 2. Original Lena image.

Fig. 3. Impulse response of the original full-order 2-D system (Example 6.1).

with a causal quarter plane ROS is fitted to this image. This model is obtained by solving a system of Yule–Walker equations. The estimates of the covariances are obtained globally. The reflection coefficients of the 2-D AR model in a window of size 4 × 4 are shown in Table I.

Based upon the eigenvalues of A_1 and A_4, which are computed to be

$$\lambda_{11} = 0.8463519, \ \lambda_{12} = \lambda_{13} = 0.4065156$$

$$\lambda'_{41} = 0.4655526, \ \lambda'_{42} = \lambda'_{43} = 0.3808155$$

and the structure of A_1 and A_4 matrices as defined in (14), ϵ was chosen to be $\epsilon = .817986$. Once ϵ is determined, the matrices in the full-order state-space model (12) can be formed using (14) and (15). The impulse response of the original full-order 2-D system is shown in Fig. 3.

With the 2-D AR model completely defined in a 2-D singularly perturbed state-space form, the transformation matrices T_1 and T_2 may be formed. However, generating T_1 and T_2 requires solving a set of Riccati and Lyapunov-type equations given in (21) and (22) iteratively. Convergent solutions for these equations are obtained in 12 and 25 steps for M_1, L_1 and M_2, L_2 pairs, respectively. Now the transformation matrices T_1 and T_2 may be formed using (16). Applying these transformation matrices T_1 and T_2 to matrices A_1 and A_4 would block diagonalize these matrices. The blocks of A_1 and A_4 are given below.

$$A_1^s = 0.8463674$$

$$A_1^f = \begin{bmatrix} 0.1894367 & 0.8179859 \\ -0.2020152 & 0. \end{bmatrix}$$

$$A_4^s = 0.4656191$$

$$A_4^f = \begin{bmatrix} -0.3116135 & 1.704438 \\ -0.1773056 & 0.5043840 \end{bmatrix}.$$

As can be seen A_1^s and A_4^s exactly capture the slow eigenvalues of A_1 and A_4 matrices, respectively. Similarly, A_1^f and A_4^f exactly capture the fast eigenvalues of A_1 and A_4. The eigenvalues of A_1^f and A_4^f are

$$\lambda_{12}^f = \lambda_{13}^f = 0.4065041$$
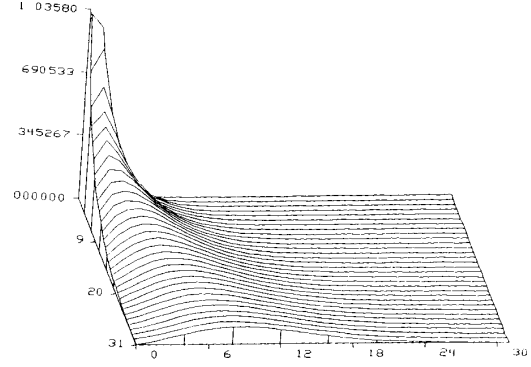
$$\lambda_{42}^f = \lambda_{43}^f = 0.3808326$$

TABLE I
THE REFLECTION COEFFICIENTS OF THE 2-D AR MODEL IN A 4 × 4 WINDOW

				q
0.001314895	−0.04401444	−0.001734353	0.06751464	3
0.03194273	0.06911532	0.07141313	−0.2347962	2
−0.09107567	0.01503638	−0.4019548	0.6583896	1
0.1398638	−0.3255982	1.035804	−1	0
p				
3	2	1	0	

Using the method developed in Section IV, the quasi-steady-state values of the fast variables are subtracted from the fast states to generate new fast states. The aggregated 2-D state-space model (43) is then formed by computing R_i's and K_i's, $i = 1, \cdots, 4$ and S_j's, $j = 1, 2$ given in (36). These matrices are then used to generate the matrices in model (43). The impulse response of this 2-D system is shown in Fig. 4. A comparison between the impulse response of the original full-order system (12) and the aggregated system (43) indicates that the behavior of the original full-order system is closely captured in this new model, except that overshoot is slightly larger in the latter response. The above full-order system may be used to generate the reduced-order 2-D subsystems (45) and (46), i.e., the slow and fast subsystems that are

$$\begin{bmatrix} \tilde{x}^{hs}(m+1, n) \\ \tilde{x}^{vs}(m, n+1) \end{bmatrix} = \begin{bmatrix} 0.8437112 & 0.0671574 \\ 0.8575461 & 0.5656865 \end{bmatrix}$$

$$\cdot \begin{bmatrix} \tilde{x}^{hs}(m, n) \\ \tilde{x}^{vs}(m, n) \end{bmatrix} + \begin{bmatrix} 0.837539 \\ 1.027984 \end{bmatrix} u(m, n)$$

$$y^s(m, n) = \begin{bmatrix} 1.375461 & 0.6261222 \end{bmatrix}$$

$$\cdot \begin{bmatrix} \tilde{x}^{hs}(m, n) \\ \tilde{x}^{vs}(m, n) \end{bmatrix} + 0.6488338 \, u(m, n)$$
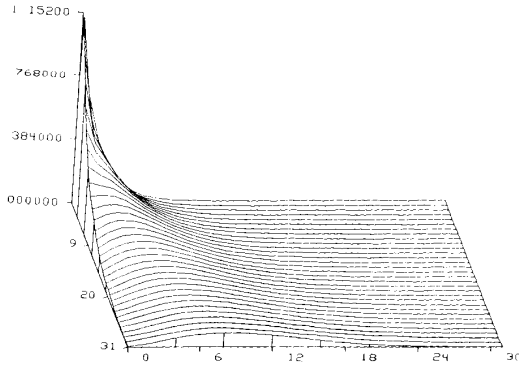
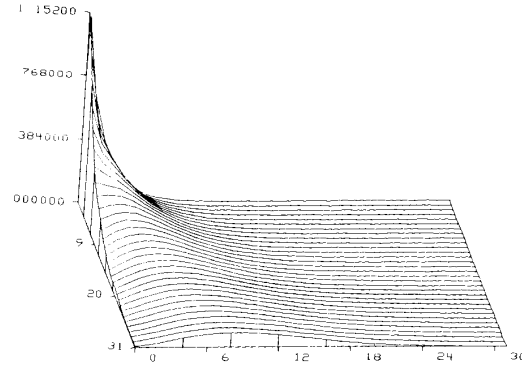Fig. 4. Impulse response of the 2-D system obtained after transformation and change of fast variables.

Fig. 5. Impulse response of the reduced-order 2-D slow subsystem (Example 6.1).

and

$$\begin{bmatrix} Z^{hf}(k+1,l) \\ Z^{vf}(k,l+1) \end{bmatrix} = \left[\begin{array}{cc|cc} 0.1894367 & 0.8179859 & -0.05375393 & 0.1106981 \\ -0.2020152 & 0.0000000 & -0.00334201 & 0.0436721 \\ \hline 3.621331 & 3.500319 & -0.3116135 & 1.704438 \\ 2.0605088 & 1.991654 & -0.1773056 & 0.504384 \end{array}\right] \begin{bmatrix} Z^{hf}(k,l) \\ Z^{vf}(k,l) \end{bmatrix}$$

$$y^f(k,l) = \begin{bmatrix} 0.6261222 & 0.01693949 & -0.1643277 & 0.0000000 \end{bmatrix} \begin{bmatrix} Z^{hf}(k,l) \\ Z^{vf}(k,l) \end{bmatrix}.$$

The fast subsystem represents a 2-D system without external excitation. Owing to the fact that fast dynamics decay very quickly, any nonzero initial condition can be brought to zero in few sampling intervals. However, since for computing an impulse response the initial conditions are set to zero, thus the fast subsystems has zero impulse response. This fact is evident from the plot of the impulse response of the reduced-order slow subsystem shown in Fig. 5, which has to be compared with the plot of the impulse response of the full-order system shown in Fig. 4. Consequently, the reduced-order slow subsystem captures the dynamical behavior of the full-order system.

To show the usefulness of the proposed model reduction scheme for image modeling and image data compression applications, we have reconstructed the girl image by passing the driving noise process through a 2-D system. First, the original full-order model is used for this reconstruction. The recovered image is shown in Fig. 6, which resembles very closely to the original Lena image in Fig. 2. Then the first-order slow subsystem is employed and the resultant reconstructed image is shown in Fig. 7. The CPU times for this reconstruction are measured to be approximately 14 min and 5 min for the full-order and the reduced-order slow subsystem models, respectively. This clearly reveals the effectiveness of the proposed scheme in image representation. This capability can be utilized in a number of image processing problems such as image data compression, image restoration, enhancement, and many other areas where 2-D linear models for the images and the filters are needed.

To compare our results with those of the conventional image data compression schemes we have employed the KL transform or the principal component method [16]. This particular algorithm is well known for its optimality in accurate data compression and its energy compaction or reduced dimensionality properties. In order to apply KL transform the image is partitioned into nonoverlapping blocks of size 8×8. The covariance matrix of size 64×64 is evaluated based upon the global statistics of the image. This matrix is then diagonalized using an orthonormal transformation. Examination of the eigenvalues shows that only 16 of 64 values are significant and thus only 16 eigenvectors corresponding to these most significant eigenvalues can be used for coding and subsequently the reconstruction. The reduced transform matrix is then used to map each individual 8×8 block to 16 KL coefficients. These coefficients can be used to reconstruct the original image from its eigen-images. The reconstructed image is shown in Fig. 8. As can be seen, the KL transform causes undesirable blocking effects that would be even more prominent, particularly around the edges, when smaller number of eigenvalues are used. To reduce this effect, smaller block size may be used. However, this would result in less accurate estimates of the covariance matrix. The CPU time for reduction and reconstruction is approximately 18 min, which is considerably higher than that of the model reduction scheme in this paper.

5.2. ARMA Modeling Example

Consider a 2-D ARMA $(2 \times 2, 31 \times 31)$ which can be represented by a cascaded of an AR(2×2) and an MA(31×31). The coefficients of the polynomial $A(z_1^{-1}, z_2^{-1})$ associ-

Fig. 6.   Reconstructed Lena image using the original full-order 2-D system.

(a)

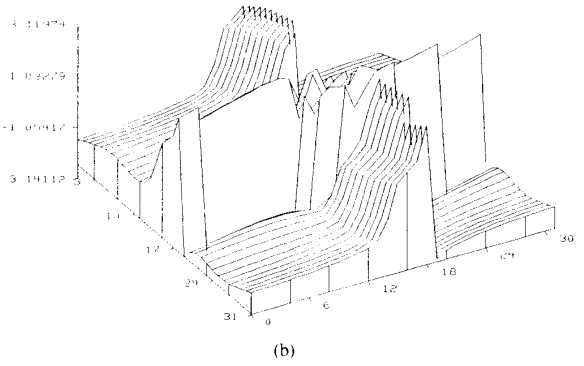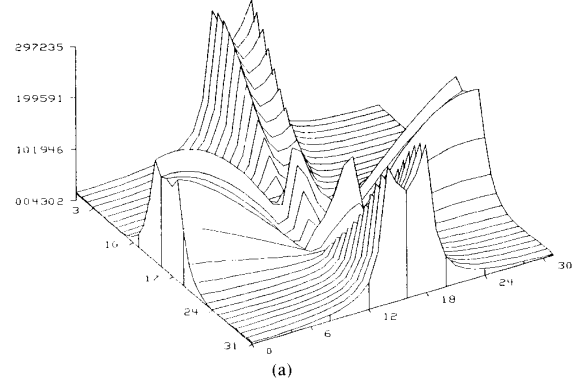Fig. 7.   Reconstructed Lena image using the reduced-order (first-order) 2-D slow subsystem.

(b)

Fig. 9.   (a) Magnitude response of the 2-D MA (31 × 31) part. (b) Phase response of the 2-D MA (31 × 31) part.

TABLE II
COEFFICIENTS OF $A(z_1^{-1}, z_2^{-1})$ IN A 3 × 3 GRID

			q
−0.02471	−0.05030	0.01802	2
−0.05030	0.00101	0.53397	1
0.01802	0.53397	−1	0
p			
2	1	0	

Fig. 8.   Reconstructed Lena image using 2-D KL transform.

ated with the AR part are shown in Table II over a 3 × 3 grid. The magnitude and the phase characteristics of the MA part are shown in Fig. 9(a) and (b), respectively. The impulse response of the overall original system is shown in Fig. 10. As pointed out in Section II, the proposed model reduction scheme is only applied to the AR part.

The eigenvalues of matrix A_1 are the roots of

$$A\left(z_1^{-1}, 0\right) = 1 - a_{10} z_1^{-1} - a_{20} z_1^{-2} = 0$$

that are $\lambda_{11} = 0.5658177$, and $\lambda_{12} = 0.03184765$. Similarly the eigenvalues of matrix A_4 are the roots of

$$A\left(0, z_2^{-1}\right) = 1 - a_{01} z_2^{-1} - a_{02} z_2^{-2} = 0$$

that are $\lambda'_{41} = 0.5658177$ and $\lambda'_{42} = 0.03184765$. Thus the perturbation parameter is set to be $\epsilon = 0.5628606$. Following the same procedure as in Example 1, the matrices in the full-order 2-D model are formed and the convergent solutions for (M_1, L_1) and (M_2, L_2) pairs are obtained, respectively, after three and four iterations of the Riccati and Lyapunov equations. The block diagonalizing transformation matrices T_1 and T_2 are then computed, which transform the full-order system into a partially decomposed 2-D state-space model. The quasi-steady-state parts of the fast variables are aggregated with the slow variables through a translation of the fast variables. This led to the following 2-D reduced-order slow
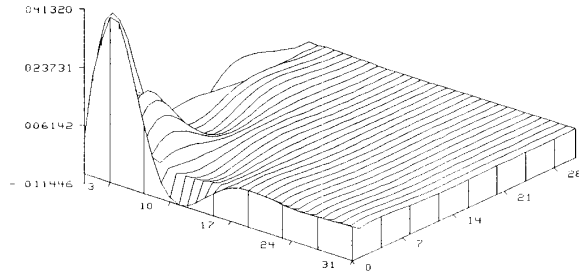
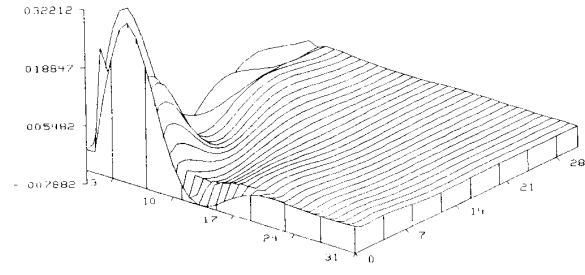Fig. 10. Impulse response of the original full-order 2-D subsystem (Example 6.2).

Fig. 11. Impulse response of the reduced-order 2-D slow subsystem (Example 6.2).

and fast subsystems:

$$\begin{bmatrix} \tilde{x}^{hs}(m+1, n) \\ \tilde{x}^{vs}(m, n+1) \end{bmatrix} = \begin{bmatrix} 0.6974283 & 0.0820584 \\ 0.8960686 & 0.6973895 \end{bmatrix}$$

$$\cdot \begin{bmatrix} \tilde{x}^{hs}(m, n) \\ \tilde{x}^{vs}(m, n) \end{bmatrix}$$

$$+ \begin{bmatrix} 0.6670664 \\ 0.8945931 \end{bmatrix} u(m, n)$$

$$y^s(m, n) = \begin{bmatrix} 0.9449549 & 0.704567 \end{bmatrix}$$

$$\cdot \begin{bmatrix} \tilde{x}^{hs}(m, n) \\ \tilde{x}^{vs}(m, n) \end{bmatrix}$$

$$- 0.05660119 \, u(m, n)$$

and

$$\begin{bmatrix} z^{hf}(k+1, l) \\ z^{vf}(k, l+1) \end{bmatrix} = \begin{bmatrix} -0.0318444 & -0.3616902 \\ 0.1663584 & -0.0318481 \end{bmatrix}$$

$$\cdot \begin{bmatrix} z^{hf}(k, l) \\ z^{vf}(k, l) \end{bmatrix}$$

$$y^f(k, l) = \begin{bmatrix} -0.09412738 & 0.0009589437 \end{bmatrix}$$

$$\cdot \begin{bmatrix} z^{hf}(k, l) \\ z^{vf}(k, l) \end{bmatrix}.$$

The impulse response of the first-order (reduced-order) 2-D slow subsystem combined with the MA part is shown in Fig. 11. As expected, the essential characteristics of the full-order 2-D system are mostly captured in the reduced-order slow subsystem.

VI. Conclusion

A decomposition–aggregation approach for a class of 2-D systems is introduced. This method is derived based upon the extension of 1-D singular perturbation methodology to the 2-D case. The strong–weak coupling effects that lead to eigenvalue clustering of A_1 and A_4 matrices in the full-order system are utilized to derive structure transformations for fast–slow decomposition. This, in conjunction with the aggregation procedure introduced in this paper, allows the

development of reduced-order 2-D slow and fast subsystems that capture the essential behavior of the full-order system. The proposed model reduction method is then applied to image modeling problems that occur in a number of image processing applications such as image restoration, image data compression, etc. The simulation results indicate the utilities of the proposed scheme.

References

[1] E. I. Jury and K. Premaratne, "Model reduction of two-dimensional systems," IEEE Trans. Circuits Syst., vol. CAS-33, pp. 558–562, May 1986.

[2] E. Badreddin and M. Mansour, "Model reduction of discrete time systems using the Schwarz canonical model," Electron. Lett., vol. 16, pp. 782–783, Sept. 1980.

[3] W. S. Lu, E. B. Lee, and Q. T. Zhang, "Model reduction for two-dimensional systems," in Proc. ISCAS '86, pp. 79–82, May 1986.

[4] A. Zilouchian and R. L. Carroll, "Model reduction of 2-D systems: A state-space approach," in Proc. 26th CDC, pp. 118–123, Dec. 1987.

[5] K. Premaratne, E. I. Jury, and M. Mansour, "Multivariable canonical forms for model reduction of 2-D discrete-time systems," IEEE Trans. Circuits Syst., vol. 37, pp. 488–501, Apr. 1990.

[6] ——, "An algorithm for model reduction of 2-D discrete time systems," IEEE Trans. Circuits Syst., vol. 37, pp. 1116–1132, Sept. 1990.

[7] M. R. Azimi-Sadjadi and K. Khorasani, "Reduced order strip Kalman filtering using singular perturbation method," IEEE Trans. Circuits Syst., vol. 37, pp. 284–290, Feb. 1990.

[8] M. R. Azimi-Sadjadi and K. Khorasani, "Application of singular perturbation for modelling image field in recursive restoration," in Proc. 26th CDC, pp. 2120–2121, Dec. 1987.

[9] ——, "Model reduction for 2-D systems," in Proc. ICASSP '89, pp. 1598–1601, May 1989.

[10] ——, "A decomposition–aggregation approach for 2-D systems," in Proc. 1990 IEEE Int. Symp. Circuits and Systems, May 1990.

[11] R. P. Roesser, "A discrete state-space model for linear image processing," IEEE Trans. Automat. Contr., vol. AC-20, pp. 1–10, Jan. 1975.

[12] P. V. Kokotovic, "A Riccati equation for block-diagonalization of ill-conditioned systems," IEEE Trans. Automat. Contr., vol. AC-20, pp. 812–814, 1975.

[13] P. V. Kokotovic, H. K. Khalil, and J. O'Reilly, Singular Perturbation Methods in Control: Analysis and Design. New York: Academic, 1986.

[14] B. Litkouhi and H. Khalil, "Multirate and composite control of two-time scale discrete time systems," IEEE Trans. Automat. Contr., vol. AC-30, pp. 645–651, July 1985.

[15] W. S. Lu and E. B. Lee, "Stability analysis for two-dimensional systems via a Lyapunov approach," IEEE Trans. Circuits Syst., vol. CAS-32, pp. 61–68, Jan. 1985.

[16] A. K. Jain, *Fundamentals of Digital Image Processing*. Englewood Cliffs, NJ: Prentice-Hall, 1989.
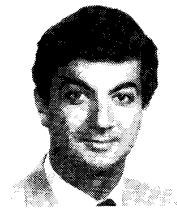
Mahmood R. Azimi-Sadjadi received the B.S. degree from University of Tehran, Iran, in 1977, and the M.S. and Ph.D. degrees from Imperial College, University of London, England, in 1978 and 1982, respectively, all in electrical engineering.

He served as an assistant professor in the Department of Electrical and Computer Engineering, University of Michigan, Dearborn. Since July 1986 he has been with the Department of Electrical Engineering, Colorado State University, where he is now an Associate Professor. His areas of interest are digital signal/image processing, multidimensional system theory and analysis, adaptive filtering, system identification, and neural networks. He is a co-author of *Digital Filtering in One and Two Dimensions* (Plenum Press, 1989).

Khashayar Khorasani (M '85) received the B.S., M.S., and Ph.D. degrees in electrical and computer engineering, all from the University of Illinois at Urbana-Champaign in 1981, 1982, and 1985, respectively.

From 1985 to 1988 he was an assistant professor at the University of Michigan, Dearborn, and since 1988 he has been at Concordia University, Montreal, Canada where he is now an Associate Professor. His current research interests are in stability and control of large-scale systems, nonlinear control, robotics, adaptive control, and neural networks. He has published more than 60 technical papers in these areas.